ISSN 0023-1584, Kinetics and Catalysis, 2006, Vol. 47, No. 1, pp. 54–63. © MAIK "Nauka/Interperiodica" (Russia), 2006.
Original Russian Text © L.O. Nindakova, F.K. Shmidt, V.V. Saraev, B.A. Shainyan, N.N. Chipanina, V.A. Umanets, L.N. Belonogova, D.-S.D. Toryashinova, 2006, published in Kinetika i Kataliz, 2006, Vol. 47, No. 1, pp. 59–68.

HIGHLY ORGANIZED CATALYTIC SYSTEMS

Formation of a Hydrogenation Catalyst in the Cobalt Acetylacetonate–Triethylaluminum System

L. O. Nindakova*, F. K. Shmidt, V. V. Saraev**, B. A. Shainyan*, N. N. Chipanina*, V. A. Umanets**, L. N. Belonogova**, and D.-S. D. Toryashinova***

** Favorskii Institute of Chemistry, Siberian Division, Russian Academy of Sciences, Irkutsk, 664033 Russia*

*** Irkutsk State University, Irkutsk, 664033 Russia*

Received November 12, 2004

Abstract—Based on the results obtained using chemical, kinetic, and physical techniques (EPR, IR, and UV spectroscopy; transmission electron microscopy; and XRD analysis), the formation of active species in the triethylaluminum–bis(tris)(acetylacetonato)cobalt system, which is known to be a hydrogenation catalyst, has been considered. It has been found that nanosized particles are formed in this system; the core of these particles consists of Co^0 atoms stabilized by a shell containing $Et_2Al(acac)$, $AlEt_3$, and their reaction products. The extremal dependence of the hydrogenation activity of the system on the Al/Co ratio is primarily due to changes in the composition of the protective shell of nanosized particles.

DOI: 10.1134/S0023158406010095

Ziegler-type systems based on transition metal complexes are widely used as efficient catalysts for the polymerization [1, 2], hydrogenation [3–5], isomerization [4–7], dimerization, and oligomerization [7–9] of unsaturated compounds. Previously [4–6, 10], it was found that catalytic systems based on organoaluminum compounds and transition metal acetylacetonates are superior to all of the known homogeneous and heterogeneous catalysts based on first-row transition metals in terms of specific activity in the hydrogenation reactions of alkenes and arenes. Ziegler *et al.* [1] hypothesized that cobalt and nickel acetylacetonates in the presence of large excesses of trialkylaluminum form colloid metal particles. However, this hypothesis was not supported in subsequent publications [3, 11]. Thus, the question concerning the homogeneous or microheterogeneous nature of the above catalytic systems is still open. Experimental data [12–14] were interpreted in terms of the formation of polynuclear complexes containing cobalt in a reduced state and organoaluminum compounds in the system; however, the structure of these species was not discussed. The mechanisms of the formation of active species and the catalytic action of the system, that is, the composition and structure of the catalyst, the oxidation state of a transition metal, and the role of triethylaluminum remain the subject of discussions.

The interaction of triethylaluminum with bis(acetylacetonato)cobalt and tris(acetylacetonato)cobalt was studied previously [15–21]. According to Dmitrieva *et al.* [21], the oxidation number of cobalt in a catalytically active species is equal to 2; however, according to Tamai *et al.* [16], Co^{2+} is reduced to Co^0.

Contradictory published data on the interaction of catalytic system components do not allow us to interpret reliably the general concepts of the effect of the composition of the system on the properties of catalysts. The formation of catalysts is still understood incompletely, although the structure of catalyst precursors has been studied using EPR [12–15], IR [16], and UV spectroscopy [15, 19, 20] to give information on a possible mechanism of the process.

Here, we report the results of a study of the $AlEt_3$–$Co(acac)_{2(3)}$ system and precipitates formed in the system in toluene and benzene solutions at various Al/Co molar ratios by EPR, UV, and IR spectroscopy; X-ray diffraction (XRD) analysis; transmission electron microscopy (TEM); and elemental analysis.

EXPERIMENTAL

Solvents and acetylacetone were purified in accordance with published procedures [22], dried, and degassed. Triethylaluminum was distilled in a vacuum (bp 48–49°C/1 Torr) and used as a 0.5 M solution in hexane. Bis(acetylacetonato)cobalt and tris(acetylacetonato)cobalt were prepared in accordance with published procedures [23]. Samples with various crystal water contents ($Co(acac)_2$, $Co(acac)_2 \cdot 0.5H_2O$, and $Co(acac)_2 \cdot 1.5H_2O$) were prepared by regulating the time of sample drying and calcination. Hydrogen was purified by passing through a nickel–chromium catalyst ($T = 350$°C) for the removal of oxygen and by freezing with liquid nitrogen in coiled pipes and passing through tubes packed with silica gel for the removal of moisture.

Alkene Hydrogenation

The reaction was performed at 20°C in a glass long-necked flask with intense shaking (300 swings per minute) using a system that allowed us to measure the consumption of hydrogen by monitoring a pressure decrease in the system. After a decrease in the pressure of hydrogen by no more than 20%, the initial pressure was restored by supplying H_2 from a buffer vessel. A portion of $Co(acac)_2$ (0.1–0.2 mmol) and 15–18 ml of a solvent were placed in a long-necked flask blown with hydrogen; a solution of $AlEt_3$ (0.2–2.0 mmol) was added dropwise from a Schlenk vessel, and 1–2 ml of an alkene was introduced. Next, the vessel was closed, the pressure of hydrogen was increased to 1–1.5 atm, the rocker was turned on, and the measurements were performed.

Sample Preparation for Studies

EPR spectroscopy. Catalytic systems were formed at 20°C in an atmosphere of argon or hydrogen in a vessel with a branch piece that allowed us to perform EPR measurements. The concentration of complexes was 10–20 mmol/l. The spectra were recorded on a Rubin spectrometer at a working frequency of 9.6 GHz 5 min after the preparation of the system at 77 K or at room temperature. The DPPH radical ($g = 2.0036 \pm 0.0003$) served as a reference substance for the determination of the g factor. The hyperfine structure (HFS) constants were calculated with the use of a signal due to Mn^{2+} in MgO.

UV spectroscopy. The reactions were performed in a vacuum (10^{-3} Torr) in glass systems connected to quartz cells with an optical path length of 0.1 cm of a Specord UV–VIS spectrometer. The UV spectra were recorded in the region 50000–28000 cm^{-1}.

IR spectroscopy. The solutions of complexes and mixtures (cobalt concentration $C_{Co} = 25$ mmol/l) were prepared in a vacuum in an atmosphere of dry argon. Next, the mixtures were transferred to a prepumped KBr cell 0.013 cm in thickness, which was filled with argon, with the use of a syringe. Solid samples were prepared by distilling toluene in a vacuum system, washing the precipitate with anhydrous hexane, and drying the samples in a vacuum (30°C/1 Torr). Dry samples were sealed in ampules in an atmosphere of argon. The IR spectra were measured on an IFS-25 spectrometer after dissolving the samples in mineral oil or pelleting them with KBr.

X-ray diffraction analysis. The XRD analysis of solid precipitates, which were prepared as in the case of IR-spectroscopic analysis, was performed on a DRON-3M diffractometer (CuK_α radiation).

Transmission electron microscopy. Micrographs were obtained on a BS-540 instrument. A catalyst solution ($C_{Co} = 5$ mmol/l) was applied to carbon-coated copper gauze in an atmosphere of argon, and the solvent was separated in the transfer chamber of the instrument.

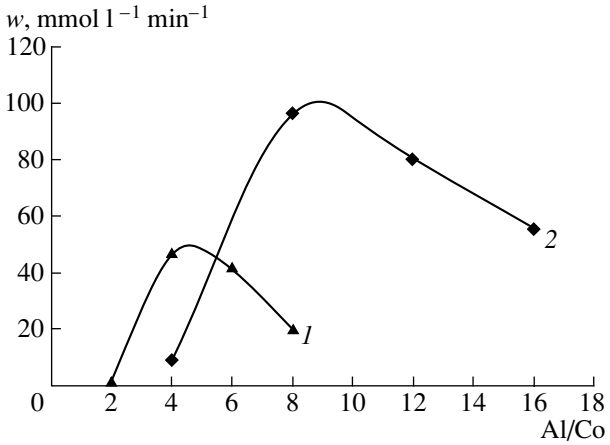

Fig. 1. Dependence of the rate of styrene hydrogenation in the $AlEt_3$–$Co(acac)_2 \cdot nH_2O$ system in toluene at 20°C on the Al/Co ratio: n = (*1*) 0 or (*2*) 1.8. $C_{Co} = 10$ mmol/l; $C_{styrene} = 1$ mol/l.

Preparation of diethylaluminum acetylacetonate. Acetylacetone (5.4 ml) was added to a solution of 55.2 mmol of $AlEt_3$ in 20 ml of decalin at –45°C for 1 h in an atmosphere of argon. The mixture was brought to room temperature with stirring and distilled in a vacuum. A pale yellow fraction with bp 68–72°C/3.5 Torr was taken. The product was poured into thin-walled glass globules and sealed. The molecular weight was $M = 310 \pm 30$, as measured by cryoscopy in benzene. ^1H NMR spectrum (δ, ppm): 0.53 (q, CH_2, J = 8.24 Hz), 1.54 (t, CH_3, J = 8.24 Hz), 1.58 (s, CH_3), and 4.95 (s, CH).

Gas-chromatographic analysis. The GLC analysis was performed on an LKhM-80 chromatograph using a column 1 m in length packed with zeolite CaA (particle size of 0.18–0.2 mm) at 20–50°C. Nitrogen or helium was the carrier gas. The liberated gas volume was calculated based on Henry's coefficients with consideration for the solubility of gas components in toluene.

RESULTS AND DISCUSSION

Hydrogenation Activity

The dependence of the catalytic activity of the $AlEt_3$–$Co(acac)_2 \cdot nH_2O$ system on the Al/Co molar ratio in the hydrogenation of alkenes exhibits an extremum (Fig. 1). The position of an extremum depends on the water content of the starting cobalt complex: in the case of an anhydrous sample, it corresponds to the ratio Al/Co = 3.5–4.0, whereas it corresponds to a ratio of 8–10 in the case of $Co(acac)_2 \cdot 1.8H_2O$. In the presence of water in the complex, the maximum rate of hydrogenation also increased (96.4 against 46.9 mmol l^{-1} min^{-1}).

The hydrogenation of 1-hexene at 20°C was accompanied by its isomerization to 2-hexene and 3-hexene;

a maximum activity was also reached at the ratio Al/Co = 3.5–4.0. However, as the concentration of cobalt was decreased, the activity maximum shifted toward higher values of Al/Co. The highest activity of the $AlEt_3$–$Co(acac)_3$ system was observed in a heptane medium at low concentrations of parent $Co(acac)_3$ (Table 1). Thus, in the hydrogenation of 1-hexene at the ratio Al/Co = 50, the catalyst turnover number (TON) in heptane (Table 1, experiment no. 2) calculated from the initial rate of hydrogenation was greater than that in toluene (Table 1, experiment no. 4) by a factor of 17.

As can be seen in Fig. 2, TON decreased with cobalt concentration, whereas the rate of reaction passed through a maximum at an optimum Al/Co ratio. Because the TON of a truly homogeneous catalyst is independent of C_{Co}, these results cannot be explained on the assumption of a homogeneous system.

Interaction between Catalytic System Components

In the interaction of $AlEt_3$ (**I**) with $Co(acac)_2$ (**II**) at C_{Co} = 5 mmol/l and Al/Co = 2–8, a visually homogeneous dark brown solution was formed; this solution did not undergo visible changes in an atmosphere of argon for 10–15 h. In the presence of crystal water in **II**, a black precipitate was formed, the yield of which increased with increasing water content of parent $Co(acac)_2$. In all cases, gas evolution was observed.

Gas evolution. The main amount of gas was released in 5 to 6 min from the mixing of reagents in toluene. The gas yield increased with Al/Co ratio and reached 3.4 and 5 mol per mole of cobalt in the case of anhydrous compound **II** and $Co(acac)_2 \cdot 0.5H_2O$ (**IIa**), respectively. Ethane, ethylene, and dimerization products of the latter (butane and butenes) were detected in the gas (Table 2).

A greater gas amount was released in a system with **IIa** because of the hydrolysis of **I** by crystal water. The formation of more than 2 mol of gaseous products per mole of cobalt in a system with **II** and a nonstoichiometric ratio between ethane and ethylene suggest that the test reaction cannot be brought to the reduction of Co^{2+} to Co^0 in accordance with the equation

$$\begin{aligned} &Co(acac)_2 + 2AlEt_3 \\ &\longrightarrow Co(0) + 2Et_2Al(acac) + C_2H_6 + C_2H_4. \end{aligned} \qquad (I)$$

A reaction analogous to reaction (I) was mentioned in previous publications [16, 24], where the degradation of organocobalt compounds with the formation of free radicals was hypothesized. However, according to our data, the yield and composition of a gas phase remained unchanged in the presence of styrene, which can quantitatively scavenge free radicals. Consequently, the process occurred without radical escape into the bulk.

The gas composition is consistent with concepts of the disproportionation of ethyl radicals formed in the system to ethane and ethylene and the dimerization of these latter to butane and isomeric butenes. The formation of ethylene and ethane in the disproportionation reaction occurred through intermediate **III** via reaction path *b* (Scheme 1). However, this does not explain the reason for excessive gas evolution. A great excess of ethane suggests the presence of additional sources of hydrogen in the system. We found that hydrogen can be abstracted from the solvent (toluene) with the formation of a benzyl derivative of Co^{2+} (**IV**) via reaction path *c*. This was supported by the fact that deuterated toluene was present in the reaction mixture after its decomposition with heavy water.

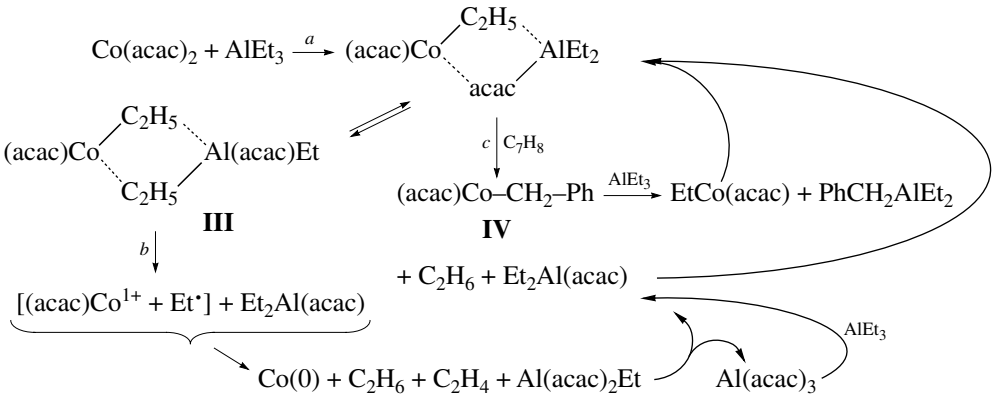

Scheme 1.

Reaction path *c* in Scheme 1 involves the formation of complex benzyl derivatives of Co^{1+} or Co^{2+} like compound **IV**, which subsequently react with **I**; as a result of this, an additional release of gaseous products occurred.

An additional source of excessive gas formation can also occur: the decomposition of **I** on Co^0 complexes with the formation of aluminum hydrides or reduced aluminum. Thus, in the decomposition of the $Co(acac)_2$ + $8AlEt_3$ system with an aqueous alkali solution after

keeping a toluene solution in an atmosphere of argon for 48 h followed by the evacuation of the solvent and released gaseous products, hydrogen (2.6%) was detected in a gas phase along with ethane (94.8%) and ethylene (2.6%). This hydrogen was liberated as the result of the hydrolysis of aluminum hydride or Al^0.

Upon the interaction of compound **I** with anhydrous **II**, the concentration of ethylene in a gas phase was much higher than that upon the interaction with **IIa**. This was likely due to the occurrence of ethylene dimerization, oligomerization, and polymerization processes at a higher rate in the latter case. This was indirectly supported by a higher concentration of dimerization and hydrodimerization products (butenes and butane) in the gas phase and by an imbalance in the total amount of ethyl groups released in a reaction between components and after the decomposition of the system with water (in particular, the deficiency of ethyl groups was 6.6 mol per mole of cobalt in the system with **II** at the ratio Al/Co = 8). The amount of ethyl groups bound to aluminum and released upon hydrolysis was 13.9 mol per mole of Co (57.5% of the initial concentration). Thus, the formation of more than 2 mol of gaseous products per mole of cobalt results from the consecutive reactions of unstable alkyl and hydride derivatives of Co^{2+} and Co^{1+} under the action of **I**.

The results of UV-, IR-, and EPR-spectroscopic and TEM studies of the $AlEt_3$–$Co(acac)_{2(3)}$ catalytic system in solutions are discussed below. The UV- and EPR-spectroscopic data were published previously [12, 15, 19, 20], and they are given here in a brief form that is sufficient for discussing the newly obtained results.

UV spectroscopy. Upon the interaction of **I** with $Co(acac)_3$ (**IIb**) in decalin (C_{Co} = 2 mmol/l) at the molar ratio Al/Co = 3, the intensity of bands at 44000 (ν_1) and 39000 cm^{-1} (ν_2) due to **IIb** decreased and the intensity of a ν_3 band due to $Al(acac)_3$ (**V**) gradually increased. The reaction was complete after 30 min. At the ratios Al/Co = 6–10, along with the ν_3 band, bands at 37300 (ν_4) and 32500 cm^{-1} (ν_5), which correspond to $Et_2Al(acac)$ (**VI**), appeared in the spectrum. In this case, the concentration ratio between **VI** and **V** was 4 : 1. The UV spectrum of the reaction mixture at the ratio Al/Co = 20 exhibited only bands due to compound **VI**; the intensity of these bands gradually decreased with time because of the degradation of an acetylacetonate chelate. Upon the addition of 2 mol of durene per mole of cobalt to a system with the ratio Al/Co = 6, compounds **VI** and **V** in a ratio of 10 : 1 appeared even after 2 min. At the ratio Al/Co = 10, the UV spectrum exhibited only bands due to **VI**; this is indicative of the stabilization of this compound in the presence of cobalt and the arene. Thus, the ratio between the products of a reaction of **IIb** with **I** depends on the Al/Co molar ratio.

Compound **VI** was formed in the reaction of **I** with one equivalent of acetylacetone. The UV spectrum of compound **VI** exhibited ν_4 and ν_5 bands; this fact suggests that the above assignment was correct. The cryoscopic determination of the molecular weight of **VI** demonstrated that this compound mainly occurred as a dimer species in benzene (M = 310 ± 30). This fact, as well as the occurrence of two bands in the UV spectrum of compound **VI** in decalin, allowed us to assume that compound **VI** also occurs as a dimer species in this medium.

Table 1. Hydrogenation of 1-hexene in the presence of the $AlEt_3$–$Co(acac)_3$ catalytic system in heptane

Experiment no.	C_{Co}, mmol/l	Al/Co	TON, min^{-1}
1	0.15	100	357
2	0.25	50	850
3	0.25	25	230
4*	0.25	50	50
5	0.50	25	200

Note: C_{Co} = 0.15–0.5 mmol/l; C_{hexene} = 1 mol/l; solution volume, 20 ml.
* In a toluene solution.

IR spectroscopy. A study of the interaction between the components of the $AlEt_3$–$Co(acac)_2$ system in benzene and toluene solutions demonstrated that the occurrence of this reaction in the above solvents did not exhibit considerable differences. Therefore, the results obtained in a benzene solution are discussed below.

At the ratio Al/Co = 2, 20 min after the mixing of reagent solutions, the intensity of absorption bands at 1592 and 1520 cm^{-1} due to ν(C=O) + ν(C=C) and ν(C=C) + ν(C=O) combined stretching vibrations in initial **II**, respectively [25], decreased and new bands at 1596 and 1530 cm^{-1} appeared (Fig. 3). The intensity of an absorption band due to ν(C–Me) + ν(C÷C) stretching vibrations at 1258 cm^{-1}, which belongs to compound **II** (10–15%) unreacted with **I**, also significantly decreased, and a band at 1291 cm^{-1} appeared due to an

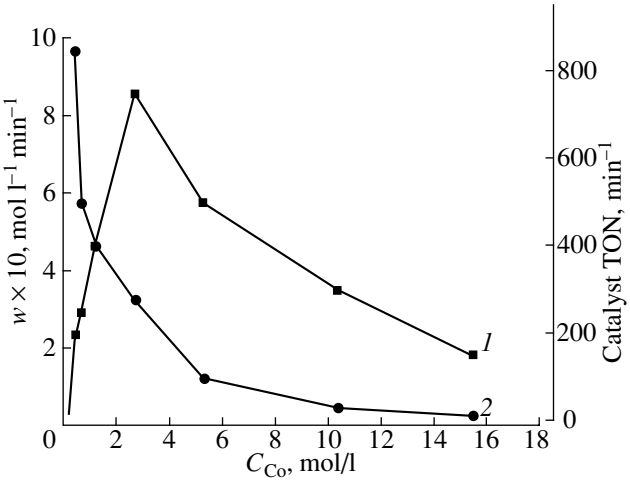

Fig. 2. Effect of cobalt concentration on (*1*) the rate of 1-hexene hydrogenation and (*2*) the catalyst TON.

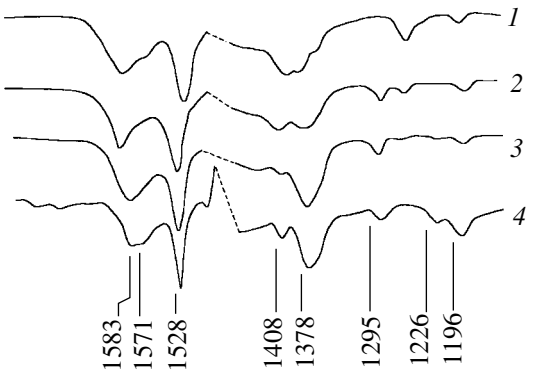

Fig. 3. IR spectra of the $AlEt_3$–$Co(acac)_{2(3)}$ catalytic system in benzene (C_{Co} = 25 mmol/l). Al/Co = (*1*) 0, (*2*) 2, (*3*) 4, or (*4*) 8. Spectra *2*–*4* were measured 20 min after mixing.

aluminum acetylacetonate compound. However, the spectrum is not the superposition of the spectra of parent compound **II** and resulting compound **VI**, because the disappearing band at 1259 cm^{-1} underwent a high-frequency shift (1264 cm^{-1}) and the band due to **I** at 1228 cm^{-1} was absent from the spectrum (Table 3). The high-frequency shift of bands in this region of the spectrum is indicative of acetylacetone binding to a center that is a stronger Lewis acid (Al as compared with Co).

The main bands of compound **V** in benzene solution appeared at 1590, 1523 (ν(C=O) + ν(C=C)), 1291 (ν(C–Me) + ν(C÷C)), and 485 cm^{-1} (δ(Al–O)) [2], and the absorption band intensity ratio δ(Al–O)/(ν(C=O) + ν(C=C)) was equal to 0.5. This compound occurred in an insignificant amount in the mixture because the above ratio was 0.14 or 0.07 20 min or 3.5 h after mixing. The latter value approaches the ratio between these absorption bands in compound **VI** (0.05). Consequently, the reaction occurred via the formation of compound **V**.

At the ratio Al/Co = 4, 20 min after the mixing of the components, the ν(C=O) + ν(C=C), ν(C=C) + ν(C=O), and ν(C–Me) + ν(C÷C) absorption bands occupied positions at 1587, 1529, and 1295 cm^{-1}, respectively, which are consistent with the set of absorption bands in **VI** (Table 3).

At the ratio Al/Co = 8, the IR spectra after 20 min exhibited the above absorption bands. However, in this case, the relative intensity of a band that appeared as a shoulder at 1570 cm^{-1} on a band at 1587 cm^{-1} (Al/Co = 4), which underwent a low-frequency shift (1585 cm^{-1}), increased. The intensity of an absorption band due to the deformation vibrations of Al–C–H bonds (1196 cm^{-1}) increased, and an absorption band appeared at ν(Al–O–C) = 1056 cm^{-1} [2] along with a band that retained its position at 1295 cm^{-1}. In the region of absorption due to the vibrations of Me–O bonds, absorption bands at 480 and 464 cm^{-1} with equal intensities were present. The shape of the IR spectrum measured 2 h after mixing coincided with that observed at the ratio Al/Co = 8 after 20 min (Fig. 3). These changes correspond to reactions shown in Scheme 2.

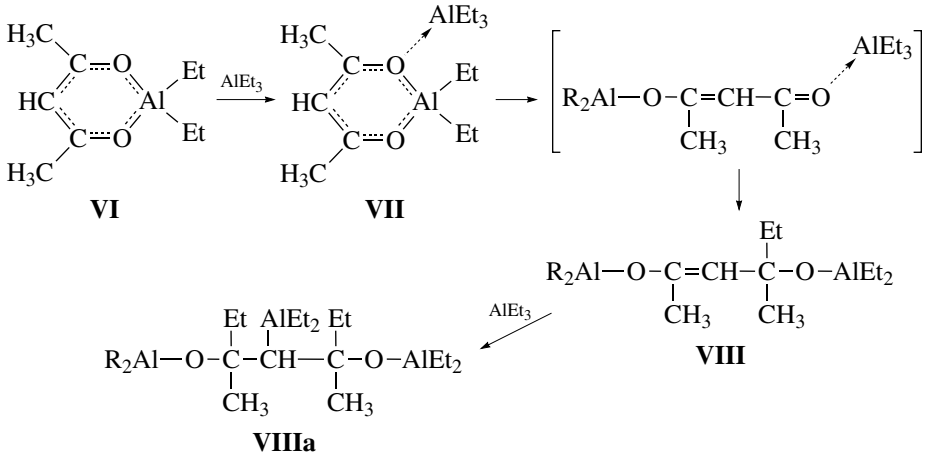

Scheme 2. Interaction of $Et_2Al(acac)$ with $AlEt_3$.

Compound **VI**, which was formed at the ratios Al/Co = 2–4, reacts with an excess of **I** with acetylacetonate chelate ring opening. The appearance and an increase in the intensity of the absorption band ν(Al–O–C) at 1056 cm^{-1} are consistent with the formation of structure **VIII**. The formation of **VIIIa** as a result of the addition of the $AlEt_3$ molecule to **VIII** is also possible. It is likely that compounds **VIII** and **VIIIa** are formed in small amounts, and the major portion of acetylacetonate groups occurred in a chelate form (as compound **VII** at the ratio Al/Co = 4–8). Bönnemann *et al.* [26] obtained nanosized colloid platinum particles coated with a shell of compounds like **VIIIa** by the reduction of $Pt(acac)_2$ under the action of $AlMe_3$. It is likely that the addition of $AlMe_3$ to $Me_2Al(acac)$ occurs more readily.

Table 2. Yields and compositions of gaseous products of the reactions of compounds **II** and **IIa** with $AlEt_3$ in toluene

Reaction with the participation of	Al/Co	Yield, mol per mole of cobalt		Product concentrations, %			
		gaseous products	ethyl groups	ethane	ethylene	butane	butenes
II	2	1.54	1.58	89.8	7.8	2.4	0.04
	4	2.12	2.16	76.1	22.3	1.1	0.6
	8*	3.42	3.54	83.7	13	2.2	1.2
IIa	1	1.9	1.96	93.0	0.3	3.0	1.5
	2	3.5	3.69	89.3	0.8	5.2	2.2
	4	4.6	5.46	75.4	1.0	14.5	6.5
	8	5.0	5.60	81.8	1.2	9.7	4.7

Note: C_{Co} = 20 mmol/l; solution volume of 20 ml.
* C_{Co} = 10 mmol/l.

Table 3. Absorption bands (cm^{-1}) of the acetylacetonate complexes of cobalt and aluminum in the IR spectra of the $nAlEt_3$–$Co(acac)_2$ system in benzene

Sample	ν(C=O)	ν(C=C)	ν(C=C) + ν(C–H)	ν(C–CH_3) + ν(C=C)	δ(Al–C–H) + δ(C–CH_3)	δ(Al–O–C)	δ(O–Al–O)
$Co(acac)_2$	1592	1520	1399, 1383, 1365	1259	1197	–	465*
$Al(acac)_3$	1590	1523	1390	1291	1186	–	487, 415
$AlEt_3$			1401, 1376		1228, 1196	–	
$AlEt_2(acac)$	1585	1530	1408, 1380	1295	1218, 1187	–	485 (w)
n = 2 (after 20 min)	1596	1530	1408, 1381	1291, 1264	1193	–	493, 464
n = 2 (after 3.5 h)	1598	1531	1408, 1393	1288, 1264	1190	–	493, 464
n = 4 (after 20 min)	1587, 1571 (sh)	1529	1408, 1378	1295	1225, 1193	1100	493, 465
n = 8 (after 20 min)	1667, 1585, 1574	1530	1408, 1378, 1324	1295	1226, 1197	1100, 1056	480, 465
n = 8 (after 135 min)	1667, 1585, 1574	1530	1408, 1378, 1324	1295	1226, 1197	1100, 1056	480, 465

Note: C_{Co} = 25 mmol/l.
* ν(Co–O) + ν(C–CH_3) [26].

EPR spectroscopy. A solution of compound **II** in toluene (C_{Co} = 10 mmol/l) did not give an EPR signal. The addition of compound **I** to the system (Al/Co = 3–5) resulted in the appearance of two signals at 77 K (Fig. 4): signal *1* with two-axis anisotropy ($g_\parallel$ = 2.344, $g_\perp$ = 2.054, $A_\parallel^{Co}$ = 6.08 mT, and $A_\perp^{Co}$ = 1.48 mT) and broad signal *2* due to the ferromagnetism of cobalt (g = 2.26; ΔH = 80 mT).

The intensity of signal *1* continuously increased with Al/Co ratio, and the concentration of the corresponding complexes became commensurable with the initial concentration of compound **II**, whereas the dependence of the intensity of signal *2* passed through a maximum. As the water content of the system was increased (to 2 mol per mole of cobalt), the intensity of signal *2* increased.

Signal *1* was observed in systems containing an initial cobalt complex with oxygen-containing ligands (acetates and salts of amino acids) and organometallic compounds of aluminum, magnesium, sodium, and lithium in the presence of arenes and in systems formed of cobalt halides in the presence of alkyl acetates or diethyl ether [27–29]. Signal *1* in the EPR spectra of the Et_3Al–$Co(acac)_{2(3)}$ system, on the one hand, and the absorption bands of compound **VI**, which is stabilized in the presence of an arene and cobalt, in the UV spectra of the above system, on the other hand, characterize the same complex of Co^0, for which the following structure of the *at* complex $[(\eta^6\text{-ArH})CoR(acac)AlEt_2]^- AlR_2^+$ was proposed:

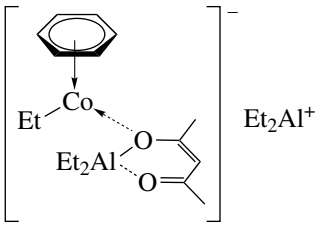

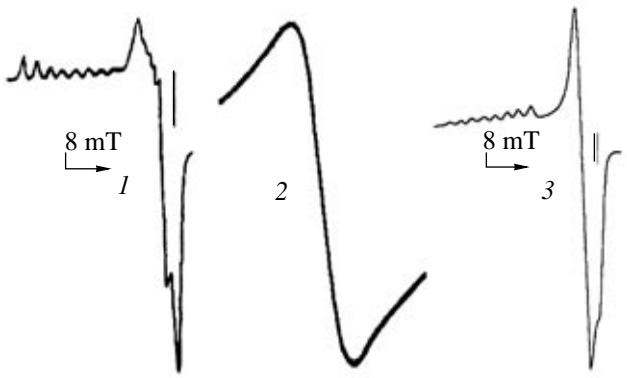

Fig. 4. EPR signals observed in the $AlEt_3$–$Co(acac)_2$ system: (*1*) the complex $[(\eta^6\text{-ArH})RCo(acac)AlEt_2]^-AlR_2^+$, (*2*) ferromagnetic Co^0, and (*3*) the complex $[(\eta^6\text{-ArH})Co(CH_2{=}CHR')(acac)AlR_2]$.

The intensity of signal *1* decreased three times and signal *3* due to a π complex of Co^0 appeared 20 min after the addition of 1-hexene to the system formed in an arene solution. This π complex of Co^0 was formed because of the displacement of an organoaluminum compound by the olefin from the coordination sphere of cobalt: $[(\eta^6\text{-ArH})Co(CH_2{=}CHR')(acac)AlR_2]$ (Fig. 4, spectrum *3*). In the course of 1-hexene hydrogenation in the Et_3Al–$Co(acac)_2 \cdot 0.5H_2O$ system (C_{Co} = 12.5 mmol/l; Al/Co = 6), signal *3* disappeared and the intensity of signal *2* and k_{eff} reached maximum values. This fact demonstrates that the alkene–arene complexes of Co^0 are the precursors of a true hydrogenation catalyst. In the course of hydrogenation, labile Co^0 complexes are transformed into ferromagnetic structures (signal *2*), which are also alkene hydrogenation catalysts.

Thus, the results obtained using EPR, IR, and UV spectroscopy demonstrate that the formation of compound **VI** and the reduction of initial Co^{2+} to Co^0 occurred in the $AlEt_3$–$Co(acac)_2$ catalytic system at the ratios Al/Co = 2–8. The subsequent appearance of broad signal *2* in the EPR spectrum was due to the manifestation of the ferromagnetic properties of cobalt.

Transmission electron microscopy. Figure 5 shows the micrographs of the $Co(acac)_2$–$AlEt_3$ system at the ratio Al/Co = 4 (C_{Co} = 5 mmol/l), which were obtained after the evaporation of a toluene solution. The sample contained primarily spherical particles from 2 to 5 nm in diameter. As can be seen in the micrographs, coarser formations of size 10–50 nm (precipitated particles) consist of smaller particles with a basic size of 5 nm. The bar diagram of a small particle size distribution exhibited two pronounced maxima at 2.6 and 5.0 nm (Fig. 6).

Thus, the interaction of catalytic system components resulted in the formation of nanosized particles

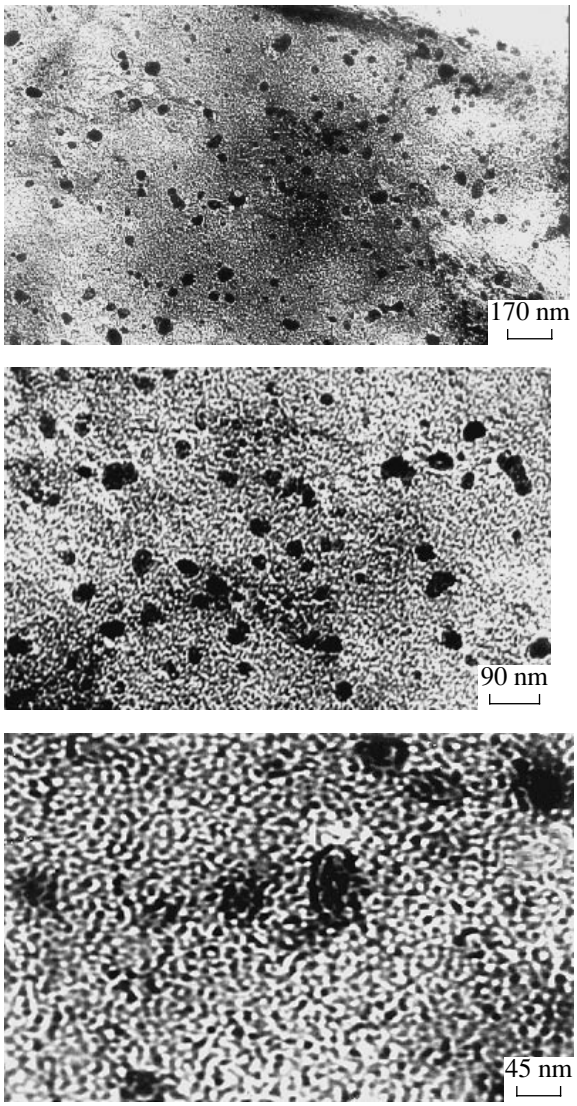

Fig. 5. Micrographs (TEM) of cobalt nanoparticles in the $AlEt_3$–$Co(acac)_2$ catalytic system in toluene (C_{Co} = 5 mmol/l; Al/Co = 4).

dispersed in toluene and likely stabilized by the resulting organoaluminum compounds and/or the solvent.

Composition and Nature of Solid Products

To determine the composition of a stabilizing shell, we studied precipitates separated from the catalytic system away from oxygen and moisture at the ratios Al/Co = 2, 4, and 8 (solvent evacuation, washing with hexane, and drying).

IR spectroscopy. The IR spectra of the precipitates (Fig. 7) also exhibited characteristic vibrational frequencies of acetylacetone bound to the aluminum atom to form a chelate (1600, 1530, and 1296–1301 cm^{-1}). In the region 600–800 cm^{-1}, a broad intense band characteristic of the vibrations of Al–O bonds was observed. Absorption bands due to Al–C (1193 and 694 cm^{-1}) and

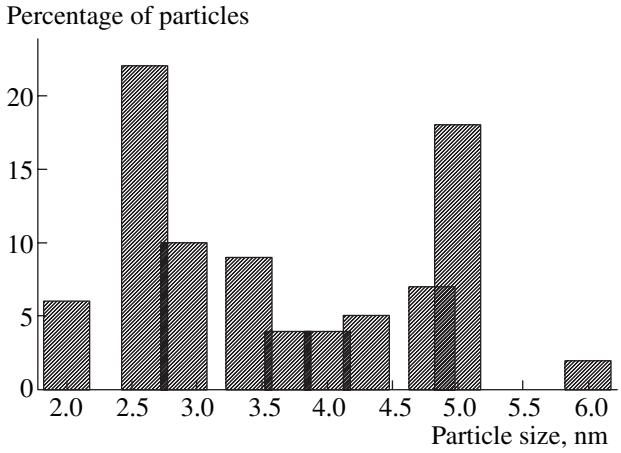

Fig. 6. Bar diagram of the particle-size distribution in the $4AlEt_3$–$Co(acac)_2$ system.

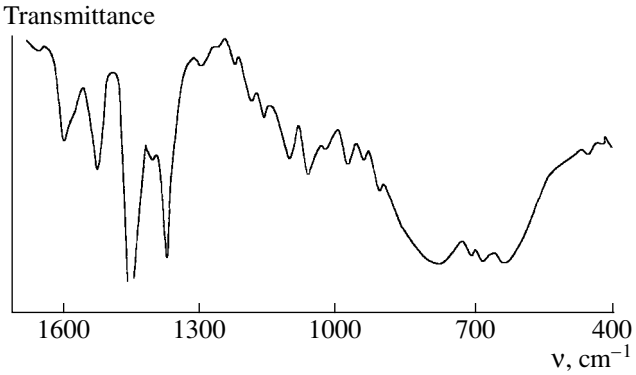

Fig. 7. IR spectrum of the precipitate separated from the $8AlEt_3$–$Co(acac)_{2(3)}$ system (in mineral oil).

Al–O bonds (1073 and 1112 cm^{-1}) were also present. A comparison between the absorption band positions of individual aluminum compounds (Table 3 and [2]) and the test samples demonstrated that the precipitates contained $Et_2Al(acac)$, alumoxanes containing the Al–O–Al bond (570–780 cm^{-1}), and a small amount of $(EtO)_2Al(acac)$ (800 cm^{-1}). The latter compound was likely formed as a result of the partial oxidation of $Et_2Al(acac)$ in the course of sample preparation for spectroscopic measurements. It is unlikely that compound **V**, for which the absorption band intensity ratio ν(Al–O)/(ν(C=O) + ν(C=C)) is equal to 0.5, was present in the precipitates, because the above ratio was no higher than 0.06 in all of the samples that exhibited an absorption band due to the vibrations of the Al–O bond.

X-ray diffraction analysis. The precipitates separated from the catalytic system with the ratio Al/Co = 4 by the above procedure exhibited a broadened diffraction line and were X-ray amorphous because of the high dispersity of particles [30]. After calcination in an atmosphere of argon at 450°C for 4 h, the samples became more crystalline, and the XRD patterns clearly exhibited lines due to four diffraction maxima with *d*/*n* 2.040 (**I**, 100), 1.773 (80), 1.253 (50), and 1.07 (50). According to Mikheev [31], these lines belong to elemental cobalt in a cubic modification (β-Co). The particle size calculated using the Selyakov–Scherrer equation [32] was ~10 nm. An additional heating of the sample at 500°C for 5 h resulted in a further narrowing of diffraction peaks, and the calculated particle size increased to ~19 nm.

We failed to detect other cobalt or aluminum compounds; this suggests that organoaluminum compounds are volatile (liquid). Note that, in the course of calcination, a viscous light yellow substance was accumulated at the top of the test tube.

Elemental analysis. Elemental analysis evidenced the presence of cobalt and aluminum with the molar ratio Al/Co = 1.88–2.2 in the precipitates. The elemental analysis of samples separated from the system at the ratios Al/Co = 2, 4, and 8 and after 1-hexene hydrogenation indicated that the concentrations of Co (17.7–18.4%), Al (16.1–17.9%), C, and H, as well as the ratios between the elements in the latter three cases, were similar (Table 4).

A comparative evaluation of the ratios between the elements in the resulting samples and organoaluminum compounds, the formulas of which are given in Table 4, demonstrated that the organoaluminum compounds are closer to alumoxanes in composition (the degree of oligomerization of 4–5). It is likely that, in the course of

Table 4. Ratio between the elements (mol/mol) in precipitates separated from the reaction products of the $AlEt_3$–$Co(acac)_{2(3)}$ catalytic system in toluene

Sample	Al/Co	C/Al	O/Al	H/C	Empirical formula of the precipitate
Al/Co = 2	0.87	7.59	4.3	1.60	$Co[Al_2C_{15.2}H_{24.4}O_{8.6}]_{0.44}$
Al/Co = 4	1.88	4.35	3.1	1.70	$Co[Al_2C_{8.7}H_{14.8}O_{5.5}]_{0.94}$
Al/Co = 8	2.20	4.23	2.39	1.99	$Co[Al_2C_{8.5}H_{16.8}O_{4.8}]_{1.1}$
After hydrogenation, Al/Co = 4	2.12	3.67	3.09	2.13	$Co[Al_2C_{7.34}H_{15.68}O_{6.2}]_{1.06}$
$[Et_2Al(acac)]_2$	–	9.0	2	1.89	$Al_2C_{18}H_{34}O_4$
Alumoxane, $n = 4$	–	6.0	2.75	1.58	$Al_4C_{24}H_{38}O_{11}$
Alumoxane, $n = 5$	–	4.8	2.9	1.55	$Al_5C_{29}H_{45}O_{14}$

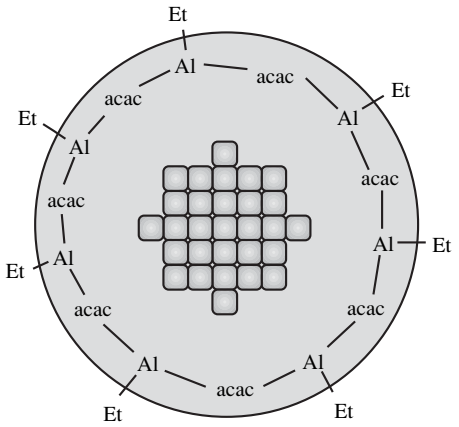

Fig. 8. Structure of a nanosized cobalt particle with a protective shell.

precipitate separation, an excess of $AlEt_3$ and $Et_2Al(acac)$, which were nonadsorbed on the surface of particles, was washed out and compound **VI** underwent partial hydrolysis.

Nature of catalytically active species. An analysis of the experimental results allowed us to generalize available information on the mechanism of formation of catalytically active particles in the $AlEt_3$–$Co(acac)_{2(3)}$ system. In the interaction of the components of the catalytic system in toluene in an atmosphere of argon, the arene complexes of Co^0, which give signal *1* in the EPR spectrum (Fig. 4), are formed. The evolution of these complexes occurs with time, and they are transformed into nanosized particles of size 2–5 nm. Compounds **I** and **VI** and the reaction products of the latter serve as a protective and stabilizing shell for cobalt metal particles. The structure of a colloid particle can be represented as follows: the core consists of elemental cobalt particles, and the shell is a "fur coat" of **I**, **VI**, and the reaction products of **VI** with an excess of **I** and toluene (Fig. 8). The ratio between the particular components of the shell depends on the concentration of compound **I** in the system. In the course of hydrogenation, signal *1* disappeared from the EPR spectrum and only signal *2* remained, which reached a maximum intensity. Ferromagnetism, which is a collective property of atoms (particles), can be observed upon the formation of clusters of cobalt metal particles, in which cobalt atoms are bound to each other by a strong exchange interaction of the ferromagnetic type. The critical size of single-domain Co particles with single-axis anisotropy is 20–25 nm [33]. The limiting size of superparamagnetic cobalt particles at 7°C was 6.4 nm [34], as found by measuring saturation magnetization and residual magnetization in systems containing Co particles with an average size of 10–15 nm. In our case, according to TEM data, the particle size of cobalt falls in a range from 2.5 to 5 nm. It is likely that coarser particles of size 10 nm or higher are responsible for the ferromagnetism of the system because a maximum intensity of signal *2* was accompanied by precipitate formation. An increase in particle size in the $AlEt_3$–$Co(acac)_2$ system prepared in an atmosphere of dry argon in anhydrous solvents at the ratio Al/Co = 4 was due to the presence of compounds **VIII** and **VIIIa** on the surface of particles and a decrease in the ability of the protective shell to prevent particle aggregation. At the above ratio Al/Co, the system exhibited the highest hydrogenation activity (Fig. 1).

Thus, the activity of the system in hydrogenation reactions, as well as the process of particle agglomeration, depends on the concentrations of components that are weakly bound to the core surface and readily displaceable from the surface by olefin molecules in the shell. It is likely that the ease of displacement decreases in the order **VIIa** > **VIII** > **VI** > **I**.

At the ratios Al/Co ≥ 8, precipitation was not observed for a long time (a few weeks). In this case, the stabilizing shell mainly consisted of the molecules of compound **I**. These molecules are prone to strong binding to electron donors because of the electron deficiency of aluminum. It is likely that the surface of a metal core meets this condition. The occurrence of such a shell prevents particle aggregation and hinders olefin coordination under conditions of catalysis; this results in a dramatic decrease or complete absence of catalytic activity (Fig. 1). Published data [35, 36] provide support for the fact that AlR_3 molecules are prone to strong binding to a metal core. In the cited publications, the synthesis of nanosized cobalt and platinum particles with stable magnetic properties and a narrow particle-size distribution was proposed with the use of the thermolysis of $Co_2(CO)_8$ in the presence of $Al(iso\text{-}Bu)_3$ [35] or the reduction of platinum in the $AlMe_3$–$Pt(acac)_2$ system [36].

The presence of crystal water in the $AlEt_3$–$Co(acac)_2 \cdot nH_2O$ system also facilitates changes in the structure of the stabilizing shell. A portion of alkyl groups in compounds **VI** and **I** is hydrolyzed to form Al–OH groups, which are capable of forming hydrogen bonds; R_2Al–O–AlR_2 alumoxanes; or the acetylacetonate derivatives of alkylalumoxanes like (acac)EtAl–O–AlR(acac) and their oligomers. These processes can be responsible for the association of Co^0 complexes, accompanied by the formation of ultradispersed colloid particles, followed by agglomeration because of a weaker bonding of shell components to the core surface. As a result, the precipitate amount and the catalytic activity in hydrogenation increased, and the position of a maximum in the plot of catalytic activity as a function of Al/Co ratio shifted toward higher values (Fig. 1).

Only broad signal *2* was observed in the EPR spectra of the catalytic systems in hexane or heptane (C_{Co} = 10 mmol/l), and a precipitate was formed. Precipitate formation was accelerated in the presence of crystal water in the samples. In this case, the formation and agglomeration of nanosized particles stabilized by organoaluminum compounds occurred much more rap-

idly because of the absence of arenes, which form mononuclear Co^0 complexes. At low cobalt concentrations (C_{Co} = 2 mmol/l), precipitation or detectable UV scattering in the wavelength region 2000–4000 Å was not observed; this is indicative of a deceleration of particle agglomeration processes. An extremely high TON of the catalyst in the hydrogenation of 1-hexene at C_{Co} = 0.25 mmol/l (Fig. 2, Table 1) supports this observation and suggests a high surface concentration of cobalt atoms accessible to catalysis, which is possible upon the formation of smaller particles.

REFERENCES

1. Ziegler, K., Gelbert, H.G., Holzkamp, E., and Wilke, G., *Ann. Chem.*, 1960, vol. 629, no. 3, p. 172.
2. Nekhaeva, L.A., Bondarenko, G.N., and Frolov, V.M., *Kinet. Katal.*, 2003, vol. 44, no. 5, p. 692.
3. Sloan, M.F., Matlack, A.S., and Breslow, D.S., *J. Am. Chem. Soc.*, 1963, vol. 85, no. 24, p. 4014.
4. Kalechits, I.V. and Shmidt, F.K., *Kinet. Katal.*, 1966, vol. 7, no. 3, p. 614.
5. Kalechits, I.V., Lipovich, V.G., and Shmidt, F.K., *Neftekhimiya*, 1966, no. 6, p. 813.
6. Stern, R. and Sajus, L., *Tetrahedron Lett.*, 1968, no. 60, p. 6313.
7. Fel'dblyum, V.Sh., Obeshchalova, N.V., and Leshcheva, A.I., *Kristallografiya*, 1967, vol. 172, no. 1, p. 111.
8. Natta, G., *Chem. Ind.*, 1965, p. 823.
9. Tembe, G.L., Bandyopadhyay, A.R., Pillai, S.M., Satish, S., and Ravindranathan, M., *Angew. Makromol. Chem.*, 1995, vol. 225, no. 1, p. 51.
10. Kalechits, I.V., Lipovich, V.G., and Shmidt, F.K., *Tezisy dokladov 4 mezhdunarodnogo kongressa po katalizu* (Proc. 4th Int. Congr. on Catalysis), Moscow, 1968, vol. 25.
11. Kroll, W.R., *J. Catal.*, 1969, vol. 15, no. 3, p. 281.
12. Saraev, V.V., Shmidt, F.K., Lipovich, V.G., and Krasnopol'skaya, S.M., *Kinet. Katal.*, 1973, vol. 14, no. 2, p. 477.
13. Shmidt, F.K., Saraev, V.V., Krasnopol'skaya, S.M., and Lipovich, V.G., *Kataliticheskie prevrashcheniya uglevodorodov* (Catalytic Conversion of Hydrocarbons), Irkutsk: Irkutsk. Gos. Univ., 1974, p. 195.
14. Saraev, V.V., Shmidt, F.K., Larin, G.M., and Lipovich, V.G., *Izv. Akad. Nauk SSSR, Ser. Khim.*, 1974, no. 11, p. 211.
15. Shmidt, F.K., Sarayev, V.V., Levkovskii, Y.S., Lipovich, V.G., Gruznykh, V.A., Ratovskii, G.V., Dmitrieva, T.V., and Nindakova, L.O., *React. Kinet. Catal. Lett.*, 1979, vol. 10, no. 2, p. 195.
16. Tamai, K., Saito, T., Uchida, Y., and Misono, A., *Bull. Chem. Soc. Jpn.*, 1965, vol. 38, no. 10, p. 1575.
17. Barrault, J., Blanchard, M., Derouault, A., Ksibi, M., and Zaki, M.I., *J. Mol. Catal.*, 1994, vol. 93, no. 3, p. 289.
18. Pasynkiewicz, S., Pietrzykowki, A., and Dowbor, K., *J. Organomet. Chem.*, 1974, vol. 78, no. 1, p. 55.
19. Ratovskii, G.V., Dmitrieva, T.V., Nindakova, L.O., and Shmidt, F.K., *Koord. Khim.*, 1980, vol. 6, no. 1, p. 61.
20. Dmitrieva, T.V., Ratovskii, G.V., Nindakova, L.O., and Shmidt, F.K., *React. Kin. Catal. Lett*, 1979, vol. 11, no. 2, p. 121.
21. Nicolesku, I.V. and Angelesku, Em., *J. Polym. Sci., Part A: Polym. Chem.*, 1966, vol. 4, no. 12, p. 2963.
22. Gordon, A.J. and Ford, R.A., *A Handbook of Practical Data, Techniques, and References*, New York: Wiley, 1972.
23. Korneev, N.N., Popov, A.F., and Krentsel', B.A., *Kompleksnye metallorganicheskie katalizatory* (Organometallic Complex Catalysts), Leningrad: Khimiya, 1969.
24. Prince, M.I. and Weiss, K., *J. Organomet. Chem.*, 1964, vol. 2, no. 2, p. 166.
25. Nakomoto, K., *Infrared and Raman Spectra of Inorganic and Coordination Compounds*, New York: Wiley, 1986.
26. Bönnemann, H., Brijoux, W., Brinkmann, R., Endruschat, U., Hofstadt, W., and Angermund, K., *Rev. Roum. Chim.*, 1999, vol. 44, nos. 11–12, p. 1003.
27. Saraev, V.V., Shmidt, F.K., Levkovskii, Yu.S., Gruznykh, V.A., Larin, G.M., and Malakhova, N.D., *Koord. Khim.*, 1979, vol. 5, no. 8, p. 1190.
28. Sarayev, V.V. and Shmidt, F.K., *J. Mol. Catal. A: Chem.*, 2000, vol. 158, no. 2, p. 149.
29. Saraev, V.V. and Shmidt, F.K., *Elektronnyi paramagnitnyi rezonans metallokompleksnykh katalizatorov* (Electronic Paramagnetic Resonance for Metal Complex Catalysts), Irkutsk: Irkutsk. Gos. Univ., 1985.
30. Kitaigorodskii, A.I., *Rentgenostrukturnyi analiz melkokristallicheskikh i amorfnykh tel* (X-ray Structure Determination for Fine-Crystal and Amorphous Solids), Moscow: Gostekhteorizdat, 1952.
31. Mikheev, V.I., *Rentgenometricheskii opredelitel' mineralov* (X-ray Diffraction Identifier of Minerals), Moscow: Gos. Nauch.–Tekh. Izd. po Geologii i Okhrane Nedr, 1957.
32. Lipson, H. and Steeple, H., *Interpretation of X-ray Powder Diffraction Patterns*, New York: Markins, 1970.
33. Petrov, Yu.I., *Fizika malykh chastits* (Physics of Small Particles), Moscow: Nauka, 1982.
34. Chernavskii, P.A., Pankina, G.V., Lermontov, A.S., and Lunin, V.V., *Kinet. Katal.*, 2003, vol. 44, no. 5, p. 718.
35. Bnnemann, H., Brijoux, W., Brinkmann, R., Matoussevitch, N., Palina, N., and Modrow, H., *Inorg. Chim. Acta*, 2003, vol. 350, no. 4, p. 617.
36. Bnnemann, H., Waldfner, N., Haubold, H.-G., and Vad, T., *Chem. Mater.*, 2002, vol. 14, no. 3, p. 1115.